materials proceedings

MDPI

Proceeding Paper

Study of Photoresistor Fabrication Based on Mercury Chalcogenides Applying Various Ligand Exchanges †

Teodora Milenkovich *, Ivan Alekseevich Shuklov, Alaa Alddin Mardini and Victor Sergeevich Popov

Moscow Institute of Physics and Technology, 9 Institutsky per., Dolgoprudny 141701, Russia; shuklov.ia@mipt.ru (I.A.S.); aladdin.mardini@phystech.edu (A.A.M.); popov.vs@mipt.ru (V.S.P.)

* Correspondence: tmilenkovich@phystech.edu; Tel.: +7-9855517448

† Presented at the 4th International Online Conference on Nanomaterials, 5–19 May 2023; Available online: https://iocn2023.sciforum.net.

Abstract: The presented paper describes the study of ligand-exchange dependent properties of mercury chalcogenides (HgS, HgTe) colloidal quantum-dot thin films. Thin films of colloidal quantum dots of mercury telluride and mercury sulfide were prepared using a layer-by-layer deposition technique applying dip-coating and spin-coating methods. The impact of the synthetic procedure of quantum dots, solvent and concentration of colloidal solution on the thin films' properties was analyzed. By using concentrated colloidal solutions in tetrachloroethylene, we succeeded in the preparation of homogeneous thin films with minimal roughness. The surface morphology and thickness of the thin films were determined using AFM. The voltage–current characteristics of photosensitive devices applying various ligand exchanges were investigated.

Keywords: mercury telluride; mercury sulfide; dip-coating; spin-coating; IV characteristics; atomic force microscopy; photoresistor

check for updates

Citation: Milenkovich, T.; Shuklov, I.A.; Mardini, A.A.; Popov, V.S. Study of Photoresistor Fabrication Based on Mercury Chalcogenides Applying Various Ligand Exchanges. *Mater. Proc.* **2023**, *14*, 21. https://doi.org/10.3390/IOCN2023-14500

Academic Editor: Ullrich Scherf

Published: 5 May 2023

1. Introduction

Colloidal quantum dots (CQDs) are nanocrystal semiconductors whose surface is covered with organic compound shell ligands. Due to the quantum dimensional effect, their optical properties depend on the diameter of the semiconductor core.

Colloidal quantum dots of mercury chalcogenides make solution-based materials which are of interest because of their mid-IR spectral range. They may have potential for making optoelectronic devices due to their low price and simple method of production [1].

Colloidal quantum dots (CQDs) of mercury telluride have attracted a lot of attention in the last decade because of their unique properties [2]. Mercury telluride-based CQDs are promising candidates for use in various fields of engineering and science due to their incomparable combination of a large radius of the Boron exciton (30 nm) and the band gap (0 eV) for bulk material. This ensures the spectral rearrangement of the properties of the CQDs from the near to far IR range. On the basis of this material photodetectors, lasers and applications in telecommunication devices are being actively developed [3–5].

Mercury sulfide CQDs are a material that has been less investigated, and based on our research, interesting results have been obtained. In comparison to mercury telluride, which is semimetal in bulk form, mercury sulfide bulk material presents a gap, and there are two crystalline forms of it (zinc blend and cinnabar) which could have chiral optical characteristics [1,2].

Photosensitive thin films are created from solutions of colloid quantum dots of mercury chalcogenide for use in photo devices. The composition of the ligand shell strongly affects the photoelectric properties of thin films [6].

The purpose of this research to fabricate photoresistors based on mercury sulfide and mercury telluride colloidal quantum dot solutions, and to define their properties. Using

atomic force microscopy (AFM) and volt-ampere characteristics (VAC) measurements, the two materials (HgTe and HgS) could be analyzed.

2. Materials and Methods

A series of experiments with application of layers of CQDs based on HgTe and HgS on glass substrates and electrodes, followed by exchange of ligands, were performed.

The application of a solution of colloidal quantum dots is carried out using dip-coating and spin-coating (35 s, 2500 rotations/min) methods. After each application of the CQDs layer, the original oleate ligand shell was replaced with the following ligands: S^{2-}, SCN^{-}, I^{-}, ethanditiol-1,2.

The procedure for changing ligands to ethanditiol-1,2 (EDT) was performed according to the following scheme.

1. The sample was placed for 30 s in a solution of EDT/HCl/isopropanol (concentration 1/1/100 in volume);
2. The sample was placed for 30 s in pure isopropanol to wash away the ligand residues from the previous stage.

Procedures for changing ligands to S^{2-}, I^{-} and SCN^{-} were carried out using an analogical method with proper solutions.

When layers of CQDs of HgTe and HgS were prepared on glass substrate, the reliefs of the surfaces of thin films were analyzed using an atomic force microscopy (AFM) method. Using AFM, the uniformity of the application of layers, the roughness of surface and the thickness of the films were determined. After determining the thickness of the layers of the samples with AFM, the procedures of application and exchange of various ligands were carried out on electrodes. Photosensitive films were created by applying layers of colloidal quantum dots of mercury chalcogenides to golden electrodes. As part of the work, measurements of both dark volt–ampere characteristics (VAC) and light VAC were made, when illuminated with a laser at 980 nm, for thin films of mercury chalcogenides. After replacing the original shells with I^{-}, S^{2-}, SCN^{-} and ethandithiol-1,2, the obtained results were analyzed.

3. Results and Discussion

Thin films were prepared based on solutions of colloidal quantum dots using four different ligand exchanges. The optical density of prepared films was measured (Figure 1).

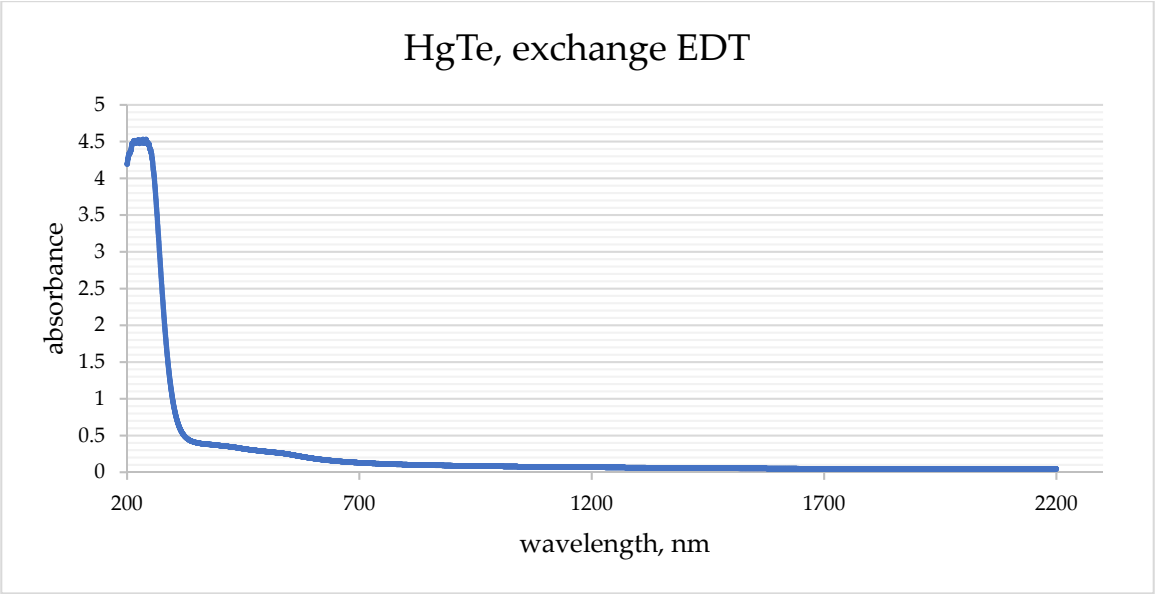

Figure 1. Optical density of thin films of five layers of HgTe with EDT ligand exchange.

The arranged thin films were analyzed using atomic force spectroscopy (AFM). AFM analysis of one of samples of HgTe CQDs is presented in Figure 2.

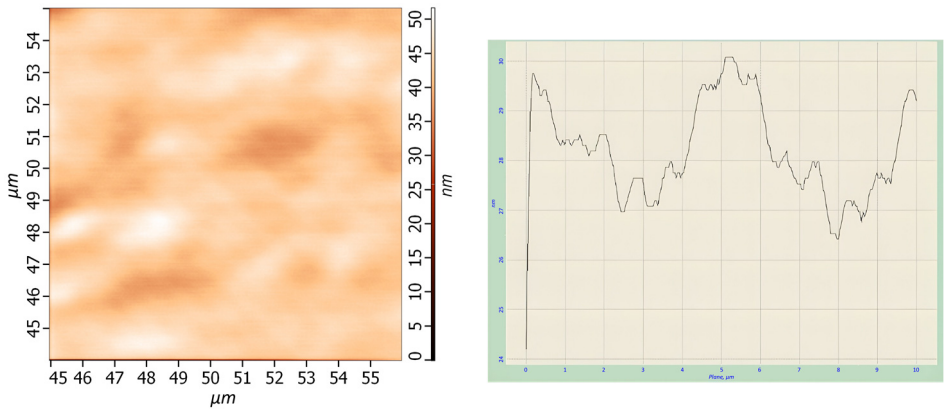

(**a**) (**b**)

Figure 2. (**a**) AFM image (10 μm × 10 μm) of thin films of five layers of HgTe with EDT ligand exchange (thickness 60 nm); (**b**) AFM analysis of the surface roughness of thin films of five layers of HgTe with EDT ligand exchange.

Based on the measurements of VAC, graphs of the current–voltage dependence for each electrode and different ligand substitution in both darkness and laser lighting conditions were constructed. In the case of HgTe, experiments were performed on each electrode in November 2021 and March 2022 to examine how the properties of photoresistors change with time. A photoresistor with ethanditiol-1,2 ligand exchange saved its properties in both experiments. In the cases of SCN^- and S^{2-} ligand exchange, the photoresistors' resistance in the dark is less than with laser lightning (November experiment), and they lost their photosensitive properties by March. The iodide-substituted photoresistor did not have photosensitivity, and its resistance did not change over time. In the case of different substitutions, the current–voltage dependence functions have different forms. A classical photosensitive element (photoresistor) with linear CV function was obtained in the case of EDT ligand exchange (Figure 3). The results of AFM and VAC measurements are shown in Table 1.

Table 1. Results of experiments with CQDs HgTe, thickness of layers and resistance of electrodes.

Quantum Dots/Ligand	Thickness of Layers (nm)	R (Laser, 980 nm) (Ω), November 2021	R (Darkness) (Ω), November 2021	R (Laser, 980 nm) (Ω), March 2022	R (Darkness) (Ω), March 2021
HgTe/S	60	1.78×10^6	1.35×10^6	1.00×10^6	1.00×10^6
HgTe/SCN	60	3.56×10^5	2.60×10^5	4.54×10^5	4.41×10^5
HgTe/TBAI	70	2.94×10^3	3.19×10^3	3.00×10^3	2.24×10^3
HgTe/EDT	60	4.26×10^2	5.54×10^2	6.00×10^2	8.67×10^2

The solutions of quantum dots of HgS were synthetized using different parameters. By combining those parameters, several different samples were used for preparing thin films, and the results of AFM analysis of them are presented in Table 2. AFM images and analysis of several samples were demonstrated on Figures 4–6.

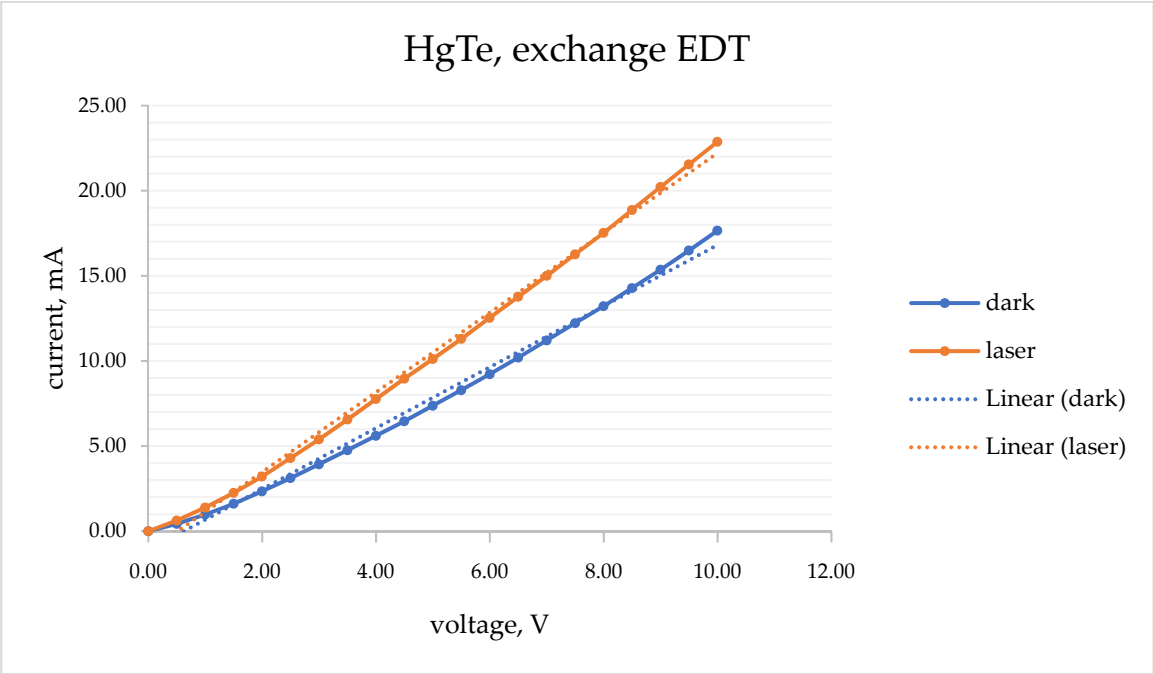

Figure 3. Graph of current–voltage characteristics of electrode with five layers of CQDs of HgTe, EDT ligand exchange.

Table 2. Results of AFM measurements of HgS CQDs thin films, with parameters used for their synthesis from $HgCl_2$/S-OLA.

Run	Time of Synthesis (min)	Solvent	Ligand Exchange	Number of Layers	AFM Analysis
1 [a]	15	Tetrachloroethylene	S^{2-}	20	Failed in making thin films
2 [b]	15	Tetrachloroethylene	S^{2-}	5/10	Roughness: 10 nm/15 nm Thickness: 50 nm/100 nm
3 [a]	15	Tetrachloroethylene	SCN^{-}	5/7	Roughness: 20 nm/30 nm Failed in making homogeneous surface of thin films
4 [a]	30	Tetrachloroethylene	S^{2-}	3/5/10	Roughness: 20 nm/30 nm/30 nm Thickness: 30 nm/50 nm/100 nm
5 [b]	60	Octane	SCN^{-}	3	Poor adhesion to glass substrate, failed in making thin films
6 [b]	15	Octane	SCN^{-}	10	Roughness: 100 nm Thickness: 100 nm

[a] low concentration of solution (10 mg/mL), [b] low concentration of solution (50 mg/mL).

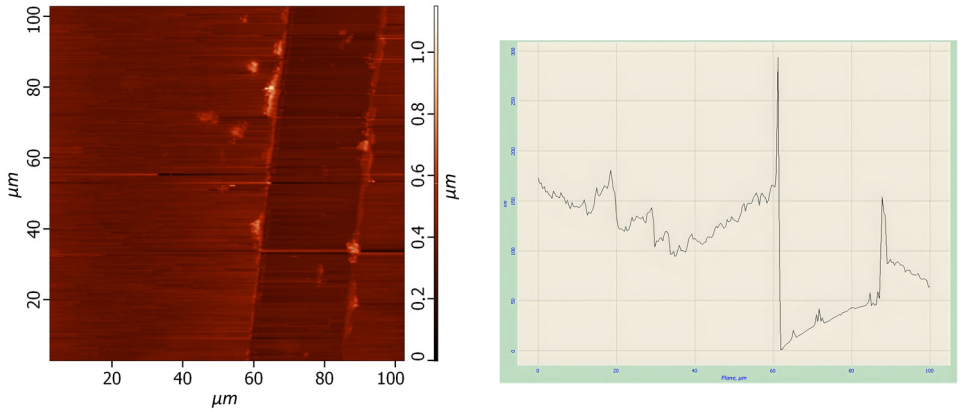

(**a**) (**b**)

Figure 4. (**a**) AFM image (100 µm × 100 µm) of thin films based on ten layers of HgS CQDs with S^{2-} ligand exchange; (**b**) AFM analysis of roughness and thickness of the thin films' surface, based on ten layers of HgS CQDs with S^{2-} ligand exchange.

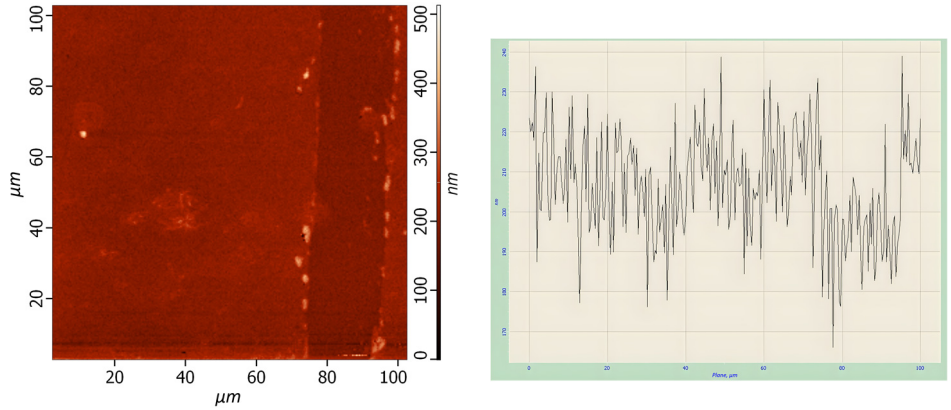

(**a**) (**b**)

Figure 5. (**a**) AFM image (100 µm × 100 µm) of thin films based on three layers of HgS CQDs with S^{2-} ligand exchange; (**b**) AFM analysis of roughness and thickness of the thin films' surface, based on three layers of HgS CQDs with S^{2-} ligand exchange.

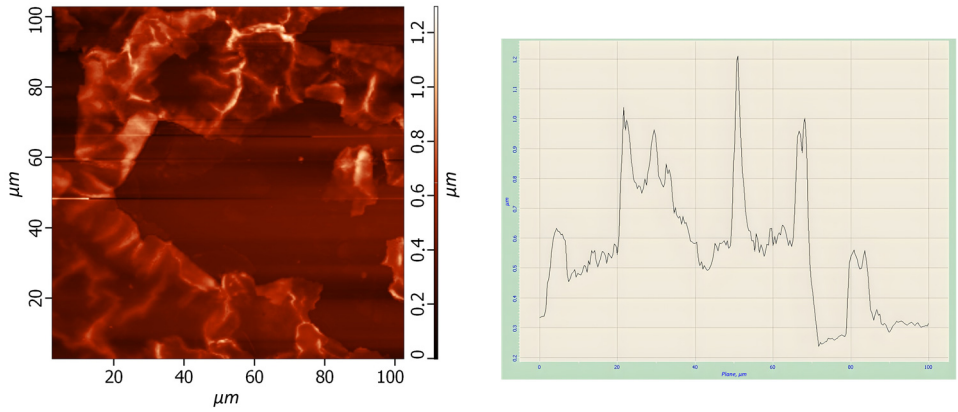

(**a**) (**b**)

Figure 6. (**a**) AFM image (100 µm × 100 µm) of thin films based on ten layers of HgS CQDs with S^{2-} ligand exchange; (**b**) AFM analysis of roughness of the thin films' surface, based on ten layers of HgS CQDs with S^{2-} ligand exchange.

4. Conclusions

In our experiments, we succeeded in producing layers of mercury chalcogenides colloidal quantum dots on glass substrates using spin-coating and dip-coating. The thin film deposition using spin-coating was optimized. The impact of the synthetic procedure of quantum dots, solvent and concentration of colloidal solution on the thin films' properties was analyzed. It was found that concentrated solutions of mercury chalcogenides in tetrachloroethylene are best suited to the preparation of homogenous thin films with a roughness below 10 nm. The proper solutions of HgTe and HgS were determined using AFM, and utilized in the preparation of photoresistors by applying layers of CQDs with various ligand exchanges on electrodes. The photoelectrical properties of photoresistors were determined, based on HgTe CQDs in the case of EDT ligand exchange, using VAC measurements.

Author Contributions: Conceptualization, T.M., I.A.S. and V.S.P.; methodology, T.M.; software, T.M.; validation, T.M., A.A.M. and I.A.S.; formal analysis, T.M.; investigation, T.M. and A.A.M.; resources, T.M.; data curation, T.M.; writing—original draft preparation, T.M.; writing—review and editing, I.A.S.; visualization, T.M.; supervision, I.A.S.; project administration, V.S.P.; funding acquisition, V.S.P. All authors have read and agreed to the published version of the manuscript.

Funding: This research was performed with the support of Ministry of Science and Higher Education of the Russian Federation, under the agreement no. 075-03-2022-207/10 dated 11 March 2022 (project No. FSMG-2022-0034).

Institutional Review Board Statement: Not applicable.

Informed Consent Statement: Not applicable.

Data Availability Statement: No new data were created or analyzed in this study. Data sharing is not applicable to this article.

Conflicts of Interest: The authors declare no conflict of interest.

References

1. Chen, M.; Guyot-Sionnest, P. Reversible Electrochemistry of Mercury Chalcogenide Colloidal Quantum Dot Films. *ACS Nano* **2017**, *11*, 4165–4173. [CrossRef]
2. Gréboval, C.; Chu, A.; Goubet, N.; Livache, C.; Ithurria, S.; Lhuillier, E. Mercury Chalcogenide Quantum Dots: Material Perspective for Device Integration. *Chem. Rev.* **2021**, *121*, 3627–3700. [CrossRef] [PubMed]
3. Keuleyan, S.; Guyot-Sionnest, P.; Delerue, C.; Guy, A. Mercury Telluride Colloidal Quantum Dots: Electronic structure, size-dependant spectra and photocurrent detection up to 12 μm. *ASC Nano* **2014**, *8*, 8676–8682. [CrossRef] [PubMed]
4. Chen, M.; Haipeng, L.; Abdelazim, N.; Zhu, Y. Mercury Telluride Quantum Dot Based Phototransistor Enabling High Sensitivity Room Temperture Photodetection at 2000 nm. *ASC Nano* **2017**, *11*, 5614–5622. [CrossRef] [PubMed]
5. Shuklov, I.A.; Razumov, V.F. Lead chalcogenide quantum dots for photoelectric devices. *Russ. Chem. Rev.* **2020**, *89*, 379–391. [CrossRef]
6. Boles, M.A.; Ling, D.; Hyeon, T.; Talapin, D.V. The surface science of nanocrystals. *Nature Mater.* **2016**, *15*, 141–153. [CrossRef] [PubMed]